Available online at www.sciencedirect.com
SCIENCE DIRECT®
Journal of Computational Physics 209 (2005) 730–753
JOURNAL OF COMPUTATIONAL PHYSICS
www.elsevier.com/locate/jcp

Geometrical integration of Landau–Lifshitz–Gilbert equation based on the mid-point rule

Massimiliano d'Aquino *, Claudio Serpico [1], Giovanni Miano [2]

Department of Electrical Engineering, University of Napoli "Federico II", via Claudio 21, I-80125 Napoli, Italy

Received 27 December 2004; received in revised form 30 March 2005; accepted 1 April 2005
Available online 23 May 2005

Abstract

Landau–Lifshitz–Gilbert (LLG) equation is the fundamental equation to describe magnetization vector field dynamics in microscale and nanoscale magnetic systems. This equation is highly nonlinear in nature and, for this reason, it is generally solved by using numerical techniques. In this paper, the mid-point rule time-stepping technique is applied to the numerical time integration of LLG equation and the relevant properties of the numerical scheme are discussed. The mid-point rule is an unconditionally stable and second order accurate scheme which preserves the fundamental geometrical properties of LLG dynamics. First, it exactly preserves the LLG property of conserving the magnetization magnitude at each spatial location. Second, for constant in time applied fields, it preserves the LLG Lyapunov structure, namely the fact that the free energy is a decreasing function of time. In addition, in the case of zero damping, the mid-point rule preserves the conservation of the system free energy. The above preservation properties are unconditionally valid, i.e. they are fulfilled for any value of the time-step. Finally, the LLG hamiltonian structure in the case of zero damping is preserved up to the third order terms with respect to the time-step. The main difficulty related to this scheme is the necessity of solving a large system of globally coupled nonlinear equations. This problem has been circumvented by using special and reasonably fast quasi-Newton iterative technique. The proposed numerical scheme is then tested on the standard micromagnetic problem no. 4. In the numerical computations, the spatial discretization is obtained by finite difference technique and the magnetostatic field is computed through the Fast Fourier Transform method.

PACS: 75.60.Jk

Keywords: Landau–Lifshitz–Gilbert equation; Micromagnetics; Geometric integration; Implicit methods; Mid-point rule; Micromagnetic standard problems

* Corresponding author. Tel.: +39 081 7683253; fax: +39 081 7683171.
E-mail addresses: mdaquino@unina.it (M. d'Aquino), serpico@unina.it (C. Serpico), miano@unina.it (G. Miano).
[1] Tel.: +39 081 7683180; fax: +39 081 7683171.
[2] Tel.: +39 081 7683250; fax: +39 081 7683171.

0021-9991/$ - see front matter
doi:10.1016/j.jcp.2005.04.001

1. Introduction

The analysis of magnetization dynamics in nanoscale ferromagnetic bodies is a very important issue from both scientific and technological points of view. A ferromagnetic body is a complex nonlinear system which may exhibit a very rich variety of dynamical behaviors including bifurcations, metastability, nonlinear resonances, quasi-periodic dynamics and spatio-temporal chaos [44]. Magnetization dynamics and relaxation, on the other hand, is one of the fundamental problems in the modern magnetic storage technologies [43]. Due to the enormous increase of data transfer rate, dynamics effects are one of the limiting factors for the performances of magnetic storage devices and materials such as hard-disk magnetic recording materials, magnetic reading sensors (magnetoresistive (MR) and giant-MR heads) [4,8], magnetic RAM elements [14,41].

The fundamental equation to describe the dynamics of magnetization vector field $\mathbf{M}(\mathbf{r}, t)$, function of the position $\mathbf{r}$ and time t, in microscale and nanoscale ferromagnetic bodies is the Landau–Lifshitz–Gilbert (LLG) equation

$$\frac{\partial \mathbf{M}}{\partial t} = -\gamma \mathbf{M} \times \left(\mathbf{H}_{\text{eff}} - \eta \frac{\partial \mathbf{M}}{\partial t} \right), \tag{1}$$

where γ is the absolute value of the gyromagnetic ratio and η is a positive phenomenological damping parameter. The vector field $\mathbf{M}(\mathbf{r}, t) \neq \mathbf{0}$ for $\mathbf{r} \in \Omega$, where Ω is the region occupied by the magnetic body. The effective field $\mathbf{H}_{\text{eff}}$ is given by the variational derivative of the micromagnetic Gibbs–Landau free energy functional $G(\mathbf{M}; \mathbf{H}_a)$ associated to the ferromagnetic body subject to an external field $\mathbf{H}_a$ [1,6,10]. More precisely, $\mathbf{H}_{\text{eff}}$ is defined as

$$\mathbf{H}_{\text{eff}} = -\frac{1}{\mu_0 V_\Omega} \frac{\delta G}{\delta \mathbf{M}}, \tag{2}$$

where μ_0 is the vacuum magnetic permeability, V_Ω is the volume of Ω, and $\delta G/\delta \mathbf{M}$ denotes the variational derivative of G with respect to $\mathbf{M}$. The meaning of $\delta G/\delta \mathbf{M}$ can be inferred from the following identity:

$$\mathrm{d}G = \int_\Omega \frac{\delta G}{\delta \mathbf{M}} \cdot \delta \mathbf{M} \, \mathrm{d}V, \tag{3}$$

where $\mathrm{d}G$ is the differential of the functional G associated to the variation $\delta \mathbf{M}$ (in the mathematical literature $\mathrm{d}G$ is usually referred to as "Frechèt derivative" of G [18]).

The functional $G(\mathbf{M}; \mathbf{H}_a)$ takes phenomenologically into account the fundamental interactions which govern magnetization processes: exchange, anisotropy, magnetostatic and Zeeman interactions. The mathematical form of $G(\mathbf{M}; \mathbf{H}_a)$ will be discussed in the sequel. For the time being, let us underline that the LLG model is the dynamic generalization of the micromagnetic theory [1,6,10], and consistently with this, it includes the assumption that $|\mathbf{M}(\mathbf{r}, t)| = M_s(T)$, namely that the magnetization vector field is assumed to have uniform magnitude within the ferromagnetic body and this magnitude is equal to the saturation magnetization $M_s(T)$ at the temperature T, which is the temperature of the body (assumed constant in time and spatially uniform) and of the heat bath surrounding it (for a justification of the micromagnetic theory see the discussion in [1]).

We notice also that, for $\eta = 0$, from Eqs. (1)–(3) one has $\mathrm{d}G/\mathrm{d}t = -\mu_0 V_\Omega \int_\Omega \mathbf{H}_{\text{eff}} \cdot \partial \mathbf{M}/\partial t \, \mathrm{d}V = 0$, and Eq. (1) describes a conservative precessional (Larmor-like) dynamics of the vector field $\mathbf{M}$ driven by the vector field $\mathbf{H}_{\text{eff}}$. As we will discuss in more details in the sequel, in the presence of damping the precessional motion of magnetization tends to relax toward micromagnetic equilibria given by the equations $\mathbf{M} \times \mathbf{H}_{\text{eff}} = \mathbf{0}$ and $|\mathbf{M}(\mathbf{r}, t)| = M_s(T)$.

Let us now turn our attention to the techniques to solve LLG equation. We shall immediately observe that, due to the nonlinear nature of this equation, analytical solutions can be derived in very few particular

cases [7,19,24,36], or by using linearization techniques (see nucleation and spin-waves problems in [1]). In fact, the only general (and mostly used) method to study magnetization dynamics is to solve LLG equation by suitable numerical methods. The most common procedure is to use a semi-discretization approach. First, the equation is only discretized in space by using finite difference or finite element methods [15]. This leads to a discretized version of the micromagnetic free energy and a corresponding system of ordinary differential equations (ODEs). Second, this system of ODEs is numerically integrated by using appropriate time-stepping techniques. It is interesting to underline that, while the spatial discretization is generally carried out trying to preserve the main properties of the energy functional $G(\mathbf{M}; \mathbf{H}_a)$, little attention is generally paid to the preservation, after the time discretization, of the peculiar structure of LLG temporal evolution. This is probably due to the fact that, in the past, the main emphasis was on static micromagnetics and on obtaining accurate approximations of the free energy landscape associated to a magnetic system subject to quasi-static external fields. This goal has been generally achieved by using sufficiently accurate spatial discretizations. On the other hand, when dynamic magnetization processes have to be investigated, the issue of using appropriate numerical time integration techniques becomes a rather crucial one. Nevertheless, this problem seems to have been substantially overlooked in magnetization dynamics studies and most workers in LLG numerical simulation use 'off-the-shelf' algorithms such as Euler, linear multi-step methods (e.g. Adams–Bashforth, Adams–Moulton, Crank–Nicholson, Backward Differentiation Formulas (BDF)) or Runge–Kutta methods [28,35]. We must underline here that these standard methods do not preserve structural properties of LLG time evolution. This equation has indeed peculiar dynamic properties, a discussion of which is in order.

(a) First, the magnetization has constant magnitude in time at each spatial location:

$$|\mathbf{M}(\mathbf{r}, t)| = |\mathbf{M}(\mathbf{r}, t_0)| \quad \forall t \geqslant t_0, \forall \mathbf{r} \in \Omega, \tag{4}$$

where the initial condition fulfills the micromagnetic constraint $|\mathbf{M}(t_0, \mathbf{r})| = M_s(T)$. Eq. (4) can be easily derived by scalar multiplying both sides of Eq. (1) by $\mathbf{M}(\mathbf{r}, t)$. It is a fundamental constraint on the LLG time evolution that should be respected in the time discretized version of LLG equation. Since usual time-stepping methods do not preserve this property, most researchers follow the naive approach of renormalizing the magnetization vector field at each time-step or after a prescribed tolerance has been exceeded. This naive approach is actually a nonlinear numerical modification of the LLG time evolution which might have relatively strong effect on the subsequent computation of magnetostatic field [21] and for this reason is not recommended, especially when long time regimes have to be studied.

(b) Second, for constant in time external field, the LLG evolution has a Lyapunov structure [30], namely the free energy functional is a decreasing function of time along the trajectories of LLG equation:

$$\frac{\mathrm{d}G}{\mathrm{d}t} = -\mu_0 V_\Omega \int_\Omega \eta \left| \frac{\partial \mathbf{M}}{\partial t} \right|^2 \mathrm{d}V, \tag{5}$$

which can be easily derived by scalar multiplying both sides of Eq. (1) by $(\mathbf{H}_{\mathrm{eff}} - \eta \partial \mathbf{M}/\partial t)$, integrating over the region Ω and using Eqs. (2) and (3). This is a fundamental property because it guarantees that the system tends toward stable equilibrium points, which are minima of free energy. Usual time-stepping techniques preserve this property only for a sufficiently small time-step. Indeed, when the time-step is too large, instability phenomena can produce transient or even steady increase of energy. The stability constraint on the time-step may usually be rather severe and this generally leads to unnecessary long computational time.

(c) Third, as previously observed, the LLG equation (1) is obtained by adding a phenomenological damping term to an otherwise hamiltonian (conservative) equation and therefore one should expect that, in the limit of $\eta \to 0$, the numerical integration should preserve energy and, if possible, the

hamiltonian structure. This is not only a mathematical requirement. In fact, in most experimental situations LLG evolution is not strongly dissipative and the damping effects can be considered as a perturbation of the conservative motion. In this respect, it is quite reasonable from the physical point of view to require that the numerical integration scheme is able to reproduce accurately the conservative motion. This is definitely the most challenging part in the numerical simulations since the conservative precession is generally much faster than the slow motion associated to dissipative processes. As it is well known in hamiltonian dynamics studies, most standard numerical schemes do not preserve energy and/or hamiltonian structure, and particular care must be devoted to develop appropriate time-stepping techniques.

As matter of fact, it is generally very difficult to obtain the preservation of the above properties in the time discretization by using explicit methods (e.g. Euler, Adams–Bashforth). Generic implicit methods (e.g. implicit Euler), on the other hand, have good performances in terms of stability, but do not generally preserve the amplitude of magnetization or the energy in the limit $\eta \to 0$. In addition, the use of implicit methods requires to solve a large system of coupled nonlinear equations at each time-step, which may lead to unacceptable computational time, if appropriate techniques to conveniently determine the solution of this system are not developed. In this respect, most researchers generally try to avoid implicit methods by using appropriate semi-implicit techniques [42]. This has of course the drawback that accurate numerical time integration requires stability upper bound for the time-step. This in turn can be quite problematic since LLG dynamics, in many relevant cases, may exhibit dynamic processes with very different time scales.

The issue of developing time integrators for LLG equation that preserve relevant properties of the equation under discretization, has received lately some attention [20,21,26,27,31,37–40]. The general point of view presented in these recent contributions is to propose the use of suitable geometric integrators [11] which are techniques designed to preserve geometrical properties of dynamics, namely symmetry, conservation of invariant quantities, hamiltonian structure etc. In particular, the possibility of developing integrators for LLG equation based on Lie-group methods and Cayley transform have been investigated in [20–22]. These methods preserve the magnetization amplitude but they do not generally preserve the LLG Lyapunov structure and the energy in the limit of zero damping. The basic idea is to take into account the conservation of magnetization magnitude by an appropriate change of variable (lift of the problem in the Lie-algebra associated to the Lie-group of rotations). The problem is then solved with usual Runge–Kutta time-stepping algorithms. These methods are conditionally stable and the stability requirements are certainly affected by the choice of the new set of state variables. This could lead to an increase of the temporal stiffness and, consequently, to an increase of the computational cost.

In this paper, we will apply the (implicit) mid-point rule to the time integration of LLG equation. We shall demonstrate that the use of mid-point rule leads to a numerical time-stepping that preserves the fundamental properties of LLG dynamics. This algorithm has been known for a long time and it has been applied extensively in the area of hamiltonian dynamics for its interesting preservation properties [3]. However, in its pure form, it has never been applied directly to the full 3D micromagnetics dynamical problem. A partial use of mid-point rule has been proposed in [37], where it has been applied along with an appropriate explicit extrapolation formula (second order Adams–Bashforth) for the effective field. This method has the property of preserving magnetization magnitude and, due to the explicit extrapolation formula, does not require the inversion of a large system of coupled nonlinear equations (but just three by three linear systems of equations at each location in space). However, the method does not in general preserve the Lyapunov structure of LLG equation neither the energy for zero damping. In addition, the semi-implicit nature of the scheme imposes stability restrictions to the time-step.

By using the mid-point rule, we can overcome the drawbacks of the standard methods. The method is unconditionally stable, preserves exactly, independently from the time-step, magnetization magnitude and, in the case of zero damping, the free energy of the system. In addition, mid-point rule preserves uncondi-

tionally Lyapunov structure of LLG dynamics for constant applied field, namely in the discrete dynamics, the free energy is always decreasing regardless of the time-step. The price we have to pay is that now we have to solve a large (generally full) system of nonlinear algebraic equations. As we will discuss in the following, this problem has been effectively tackled by using a quasi-Newton algorithm, which allows one to deal with sparse banded matrix inversions only.

2. The mathematical model

It is very useful and insightful for the following discussion to introduce a dimensionless form of LLG equation. By dividing both sides of Eq. (1) by γM_s^2, LLG equation can be written in the following normalized form:

$$\frac{\partial \mathbf{m}}{\partial t} = -\mathbf{m} \times \left(\mathbf{h}_{\text{eff}}(\mathbf{m}, t) - \alpha \frac{\partial \mathbf{m}}{\partial t} \right), \tag{6}$$

where $\mathbf{m}(\mathbf{r}, t) = \mathbf{M}(\mathbf{r}, t)/M_s$ ($m(\mathbf{r}, t) \neq 0$ for $\mathbf{r} \in \Omega$), M_s is the saturation magnetization (the dependence on the temperature is understood), $\mathbf{h}_{\text{eff}} = \mathbf{H}_{\text{eff}}/M_s$, $\alpha = \eta\gamma M_s$ is the dimensionless Gilbert damping constant, and the time is measured in units of $(\gamma M_s)^{-1}$ (where $\gamma = 2.21 \times 10^5$ Hz $(\text{A/m})^{-1}$).

The LLG equation (6) is implicit with respect to $\partial\mathbf{m}/\partial t$ and it can be transformed in the equivalent Landau–Lifshitz form:

$$\frac{\partial \mathbf{m}}{\partial t} = -\frac{1}{1+\alpha^2}\mathbf{m} \times \mathbf{h}_{\text{eff}}(\mathbf{m}, t) - \frac{\alpha}{1+\alpha^2}\mathbf{m} \times (\mathbf{m} \times \mathbf{h}_{\text{eff}}(\mathbf{m}, t)), \tag{7}$$

where $\partial\mathbf{m}/\partial t$ is explicitly expressed. This form of LLG equation is the most commonly used for numerical integration.

The normalized effective field $\mathbf{h}_{\text{eff}}$ can be defined by the variational derivative $\mathbf{h}_{\text{eff}} = -\delta g/\delta\mathbf{m}$ of the normalized micromagnetic free energy [1] functional $g(\mathbf{m}; \mathbf{h}_a) = G(\mathbf{M}; \mathbf{H}_a)/(\mu_0 M_s^2 V_\Omega)$. The functional g is formed by the sum of normalized exchange, magnetostatic, anisotropy and Zeeman energy, respectively:

$$g(\mathbf{m}; \mathbf{h}_a) = \frac{1}{V_\Omega} \int_\Omega \left[\frac{A}{\mu_0 M_s^2} (\nabla \mathbf{m})^2 - \frac{1}{2}\mathbf{h}_m \cdot \mathbf{m} + \frac{K_1}{\mu_0 M_s^2} \left[1 - (\mathbf{m} \cdot \mathbf{e}_{an})^2 \right] - \mathbf{h}_a \cdot \mathbf{m} \right] \mathrm{d}V, \tag{8}$$

where A is the exchange constant, K_1 is the uniaxial anisotropy constant, $\mathbf{e}_{an}$ is the easy axis unit-vector and $\mathbf{h}_m$ is the magnetostatic (demagnetizing) field, which is the solution of the following boundary value problem:

$$\nabla \cdot \mathbf{h}_m = -\nabla \cdot \mathbf{m}, \quad \nabla \times \mathbf{h}_m = \mathbf{0}, \tag{9}$$

$$\mathbf{n} \times [\mathbf{h}_m]_{\partial\Omega} = \mathbf{0}, \quad \mathbf{n} \cdot [\mathbf{h}_m]_{\partial\Omega} = \mathbf{n} \cdot \mathbf{m}. \tag{10}$$

In Eqs. (9)–(10), we have denoted with $\mathbf{n}$ the outward normal to the boundary $\partial\Omega$ of the magnetic body, and with $[\mathbf{h}_m]_{\partial\Omega}$ the jump of the vector field $\mathbf{h}_m$ across $\partial\Omega$.

The magnetization $\mathbf{m}(\mathbf{r}, t)$ is also assumed to satisfy the following condition at the body surface:

$$\frac{\partial \mathbf{m}}{\partial \mathbf{n}} = \mathbf{0}, \tag{11}$$

which is the condition expected when no surface anisotropy is present [1].

By considering the variational derivative of $g(\mathbf{m}; \mathbf{h}_a)$ (see Eq. (8)) with respect to the vector field $\mathbf{m}$ and by using Eqs. (9)–(10) and the boundary condition (11), one can readily derive that the effective field is con-

stituted by the sum of four terms: the exchange field $\mathbf{h}_{ex}$, the magnetostatic field $\mathbf{h}_m$, the anisotropy field $\mathbf{h}_{an}$ and the applied field $\mathbf{h}_a$:

$$\mathbf{h}_{eff}(\mathbf{m},t) = -\frac{\delta g}{\delta \mathbf{m}} = \mathbf{h}_{ex} + \mathbf{h}_m + \mathbf{h}_{an} + \mathbf{h}_a(t), \tag{12}$$

where the explicit dependence of $\mathbf{h}_{eff}$ on time is related to the dependence on time of $\mathbf{h}_a$. The first three terms in Eq. (12) are linearly related to the vector field $\mathbf{m}$ through the following equations [1]:

$$\mathbf{h}_{ex} = \frac{2A}{\mu_0 M_s^2}\nabla^2\mathbf{m}(\mathbf{r},t), \tag{13}$$

$$\mathbf{h}_m = -\frac{1}{4\pi}\nabla_{\mathbf{r}}\int_{\Omega}\nabla_{\mathbf{r}'}\left(\frac{1}{|\mathbf{r}-\mathbf{r}'|}\right)\cdot\mathbf{m}(\mathbf{r}',t)\,dV_{\mathbf{r}'}, \tag{14}$$

$$\mathbf{h}_{an} = \frac{2K_1}{\mu_0 M_s^2}\mathbf{e}_{an}(\mathbf{r})(\mathbf{e}_{an}(\mathbf{r})\cdot\mathbf{m}(\mathbf{r},t)). \tag{15}$$

From Eqs. (9)–(11) and (13)–(15), one can easily prove that the sum of the first three terms of the effective field (12) is a linear and formally self-adjoint operator acting on the vector field $\mathbf{m}$ in a suitable subspace of sufficiently regular vector fields of $\mathbb{L}^2(\Omega)$ (i.e. the space of vector fields $\mathbf{v}$ with $|\mathbf{v}|^2$ integrable) with respect to the usual scalar product in $\mathbb{L}^2(\Omega)$:

$$(\mathbf{v},\mathbf{w})_{\mathbb{L}^2(\Omega)} = \int_{\Omega}\mathbf{v}(\mathbf{r})\cdot\mathbf{w}(\mathbf{r})\,dV, \tag{16}$$

where $\mathbf{v}$ and $\mathbf{w}$ are two $\mathbb{L}^2(\Omega)$ generic vector fields. In other terms, the effective field (12) can be written in the following form:

$$\mathbf{h}_{eff}(\mathbf{m},t) = -\mathscr{C}\mathbf{m} + \mathbf{h}_a(t), \tag{17}$$

where $\mathscr{C}$ is a linear formally self-adjoint integro-differential operator in $\mathbb{L}^2(\Omega)$, namely $(\mathscr{C}\mathbf{v},\mathbf{w})_{\mathbb{L}^2(\Omega)} = (\mathbf{v},\mathscr{C}\mathbf{w})_{\mathbb{L}^2(\Omega)}$ for all sufficiently regular vector fields $\mathbf{v}$ and $\mathbf{w}$.

Let us now summarize the fundamental properties of LLG dynamics in the normalized quantities introduced above.

The first fundamental property is the normalized version of Eq. (4):

$$|\mathbf{m}(\mathbf{r},t)| = |\mathbf{m}(\mathbf{r},t_0)| \quad \forall t \geqslant t_0,\ \forall \mathbf{r}\in\Omega, \tag{18}$$

where in micromagnetics problems it is normally assumed $|\mathbf{m}(\mathbf{r}, t_0)| = 1$, which is equivalent to the micromagnetic constraint $|\mathbf{M}| = M_s$.

The second fundamental property, as preliminarily discussed in the introduction, is related to the nature of the energy balance in LLG dynamics. By scalar multiplying both sides of Eq. (6) by $(\mathbf{h}_{eff}(\mathbf{m}, t) - \alpha\partial\mathbf{m}/\partial t)$ and using the fact that $\mathbf{h}_{eff} = -\delta g/\delta\mathbf{m}$, one readily obtains the following energy balance equation:

$$\frac{d}{dt}g(\mathbf{m}(t);\mathbf{h}_a(t)) = -\int_{\Omega}\alpha\left|\frac{\partial\mathbf{m}}{\partial t}\right|^2 dV - \int_{\Omega}\mathbf{m}\cdot\frac{\partial\mathbf{h}_a}{\partial t}dV. \tag{19}$$

Let us discuss in more details the implications of this equation. First we notice that, for constant applied field, Eq. (19) reduces to

$$\frac{d}{dt}g(\mathbf{m}(t);\mathbf{h}_a(t)) = -\int_{\Omega}\alpha\left|\frac{\partial\mathbf{m}}{\partial t}\right|^2 dV, \tag{20}$$

which is the normalized version of Eq. (5). This equation shows that the LLG dynamics has a Lyapunov structure [30], namely, for constant external field, the free energy is always a decreasing function of time. In

addition, it also demonstrates the nature of the Gilbert phenomenological damping: the dissipation is given by a quadratic form of the vector field $\partial\mathbf{m}/\partial t$. This is connected to the fact that the Gilbert damping term can be introduced by using a Rayleigh dissipation function given by $(1/2)\int_\Omega \alpha|\partial\mathbf{m}/\partial t|^2\,\mathrm{d}V$ [16,17].

The property expressed in Eq. (20) is very important because it guarantees that, under constant external field, the system tends toward meta-stable equilibrium states, which are the minima of the free energy. This property strongly limits the possible dynamics of LLG equation under constant external conditions since it prevents the emergence of self-oscillations or chaotic behaviour. These more complicated dynamical behaviours can be driven only by means of time-varying external fields [44].

The third fundamental property is related to the structure of the equation when $\alpha = 0$. In this case, the LLG equation becomes an hamiltonian dynamical system for the vector field $\mathbf{m}$ defined as

$$\frac{\partial\mathbf{m}}{\partial t} = \mathbf{m}\times\frac{\delta g(\mathbf{m};\mathbf{h}_\mathrm{a})}{\delta\mathbf{m}}. \tag{21}$$

The LLG hamiltonian form (21) is not the ordinary hamiltonian form with positions and conjugate momenta evolution equations. This form belongs to a more general class of hamiltonian equations which can be defined by introducing an appropriate Poisson bracket [25]. In the case of Eq. (21), the associated to LLG Poisson bracket is given by the following Lie–Poisson bracket [9]:

$$\{f(\mathbf{m}),h(\mathbf{m})\} = -\mathbf{m}\cdot\frac{\delta f}{\delta\mathbf{m}}\times\frac{\delta h}{\delta\mathbf{m}}, \tag{22}$$

where $f(\mathbf{m})$ and $h(\mathbf{m})$ are two generic functionals of $\mathbf{m}$. In Eq. (21), the role of the hamiltonian is played by $g(\mathbf{m};\mathbf{h}_\mathrm{a})$ and it can be written as

$$\frac{\partial m_x}{\partial t} = \{m_x, g(\mathbf{m};\mathbf{h}_\mathrm{a})\},\quad \frac{\partial m_y}{\partial t} = \{m_y, g(\mathbf{m};\mathbf{h}_\mathrm{a})\},\quad \frac{\partial m_z}{\partial t} = \{m_z, g(\mathbf{m};\mathbf{h}_\mathrm{a})\}. \tag{23}$$

It should be underlined that, although the LLG dynamics is always dissipative, it is interesting to consider the conservative case since in most experimental situations the dissipative effects are quite small (typically $\alpha \ll 1$). In other terms, the LLG dynamics, on relatively short time scale, is a perturbation of the conservative (hamiltonian) precessional dynamics.

3. Spatially semi-discretized LLG equation

We now introduce a spatially discretized version of the mathematical model (6). The discussion presented below is considerably general and thus applicable to all the usual spatial discretization techniques such as finite difference or finite elements [15].

To start the discussion, let us assume that the magnetic body has been subdivided in N cells or finite elements. We denote the magnetization vector associated to the lth cell or node by $\mathbf{m}_l(t) \in \mathbb{R}^3$. Analogously, the effective and the applied fields at each cell will be denoted by the vectors $\mathbf{h}_{\mathrm{eff},l}(t)$, $\mathbf{h}_{\mathrm{a},l}(t)$. In addition to the cell vectors, we introduce mesh vectors which are $\mathbb{R}^{3N}$ vectors formed by the collection of all cell vectors. In this respect, we will indicate the mesh vectors associated to $\mathbf{m}$, $\mathbf{h}_\mathrm{eff}$, $\mathbf{h}_\mathrm{a}$ with the notation $\underline{\mathbf{m}}$, $\underline{\mathbf{h}}_\mathrm{eff}$, $\underline{\mathbf{h}}_\mathrm{a}$. These vectors are given by

$$\underline{\mathbf{m}} = \begin{pmatrix}\mathbf{m}_1\\ \vdots\\ \mathbf{m}_N\end{pmatrix},\quad \underline{\mathbf{h}}_\mathrm{eff} = \begin{pmatrix}\mathbf{h}_{\mathrm{eff},1}\\ \vdots\\ \mathbf{h}_{\mathrm{eff},N}\end{pmatrix},\quad \underline{\mathbf{h}}_\mathrm{a} = \begin{pmatrix}\mathbf{h}_{\mathrm{a},1}\\ \vdots\\ \mathbf{h}_{\mathrm{a},N}\end{pmatrix}. \tag{24}$$

Usual spatial discretization techniques [15] (e.g. finite element and finite difference methods) quite naturally lead to a discretized version of the free energy (8), which has generally the form

$$\underline{g}(\underline{\mathbf{m}}, \underline{\mathbf{h}}_{\mathrm{a}}) = \frac{1}{2}\underline{\mathbf{m}} \cdot \underline{C} \cdot \underline{\mathbf{m}} - \underline{\mathbf{h}}_{\mathrm{a}} \cdot \underline{\mathbf{m}}, \tag{25}$$

where $\underline{C}$ is now a $3N \times 3N$ symmetric matrix[35] which describes exchange, anisotropy and magnetostatic interactions. Once the free energy has been discretized, the corresponding spatially discretized effective field $\underline{\mathbf{h}}_{\mathrm{eff}}(\underline{\mathbf{m}}, t)$ can be obtained as

$$\underline{\mathbf{h}}_{\mathrm{eff}}(\underline{\mathbf{m}}, t) = -\frac{\partial \underline{g}}{\partial \underline{\mathbf{m}}} = -\underline{C} \cdot \underline{\mathbf{m}} + \underline{\mathbf{h}}_{\mathrm{a}}(t). \tag{26}$$

We notice that the mathematical structure of the effective field (see Eq. (17)) is formally preserved after the spatial discretization, and the matrix $\underline{C}$ is the discretized version of the formally self-adjoint integro-differential operator $\mathscr{C}$.

The matrix $\underline{C}$ can be naturally decomposed into the sum of the three terms $\underline{C}_{\mathrm{ex}}$, $\underline{C}_{\mathrm{m}}$, $\underline{C}_{\mathrm{an}}$, which correspond to discretized exchange, magnetostatic and anisotropy interactions:

$$\underline{C} = \underline{C}_{\mathrm{ex}} + \underline{C}_{\mathrm{m}} + \underline{C}_{\mathrm{an}}. \tag{27}$$

It is important to observe that $\underline{C}_{\mathrm{ex}}$ and $\underline{C}_{\mathrm{an}}$ are sparse matrices since the exchange and anisotropy interactions have a local character, whereas $\underline{C}_{\mathrm{m}}$ is a full matrix owing to the long-range magnetostatic interactions.

By using the above notations, the spatially semi-discretized LLG equation consists in a system of $3N$ ODEs, which, for the generic lth cell, can be written in the following form:

$$\frac{\mathrm{d}}{\mathrm{d}t}\mathbf{m}_l = -\mathbf{m}_l \times \left[\mathbf{h}_{\mathrm{eff},l}(\underline{\mathbf{m}}, t) - \alpha \frac{\mathrm{d}}{\mathrm{d}t}\mathbf{m}_l\right], \tag{28}$$

and for the whole collection of cells as

$$\frac{\mathrm{d}}{\mathrm{d}t}\underline{\mathbf{m}} = -\underline{\Lambda}(\underline{\mathbf{m}}) \cdot \left[\underline{\mathbf{h}}_{\mathrm{eff}}(\underline{\mathbf{m}}, t) - \alpha \frac{\mathrm{d}}{\mathrm{d}t}\underline{\mathbf{m}}\right], \tag{29}$$

where $\underline{\Lambda}(\underline{\mathbf{m}})$ is a block-diagonal matrix

$$\underline{\Lambda}(\underline{\mathbf{m}}) = \mathrm{diag}(\Lambda(\mathbf{m}_1), \ldots, \Lambda(\mathbf{m}_N)) \tag{30}$$

with blocks $\Lambda(\cdot) \in \mathbb{R}^{3\times 3}$ such that $\Lambda(\mathbf{v}) \cdot \mathbf{w} = \mathbf{v} \times \mathbf{w}\ \forall \mathbf{v}, \mathbf{w} \in \mathbb{R}^3$. We also observe that $\underline{\Lambda}(\underline{\mathbf{m}})$ is linearly dependent on $\underline{\mathbf{m}}$ through an appropriate third order tensor $\underline{\Gamma}$ as

$$\underline{\Lambda}(\underline{\mathbf{m}}) = \underline{\Gamma} \cdot \underline{\mathbf{m}}, \tag{31}$$

where $\underline{\Gamma}$ is block diagonal with N diagonal $3 \times 3 \times 3$ blocks constituted by third order permutation tensors and the dot product in Eq. (31) represents an index contraction. The meaning of this contraction can be inferred by considering that the component of the vector $\underline{\mathbf{v}} \cdot (\underline{\Gamma} \cdot \underline{\mathbf{w}})$ corresponding to the lth cell is given by

$$(\underline{\mathbf{v}} \cdot (\underline{\Gamma} \cdot \underline{\mathbf{w}}))_l = \mathbf{v}_l \times \mathbf{w}_l, \tag{32}$$

where we have used the notation introduced above for mesh vectors $\underline{\mathbf{v}}$, $\underline{\mathbf{w}}$ and cell vectors $\mathbf{v}_l$, $\mathbf{w}_l$.

Now, we briefly summarize the properties of the semi-discretized LLG (28) and (29). These properties are completely analogous to the properties (18)–(22) and the demonstration can be obtained by following the very same line of reasoning. Indeed, one can easily prove that

$$|\mathbf{m}_l(t)| = |\mathbf{m}_l(t_0)| \quad \forall t \geqslant t_0,\ l = 1, \ldots, N, \tag{33}$$

$$\frac{\mathrm{d}}{\mathrm{d}t}\underline{g}(\underline{\mathbf{m}}(t); \underline{\mathbf{h}}_{\mathrm{a}}(t)) = -\alpha\left|\frac{\mathrm{d}\underline{\mathbf{m}}}{\mathrm{d}t}\right|^2 - \underline{\mathbf{m}} \cdot \frac{\mathrm{d}\underline{\mathbf{h}}_{\mathrm{a}}}{\mathrm{d}t} = -\sum_{l=1}^{N} \alpha\left|\frac{\mathrm{d}\mathbf{m}_l}{\mathrm{d}t}\right|^2 - \sum_{l=1}^{N} \mathbf{m}_l \cdot \frac{\mathrm{d}\mathbf{h}_{\mathrm{a},l}}{\mathrm{d}t}, \tag{34}$$

and, in the case of constant applied field, that

$$\frac{\mathrm{d}}{\mathrm{d}t}\underline{g}(\underline{\mathbf{m}}(t);\underline{\mathbf{h}}_{\mathrm{a}}(t)) = -\alpha\left|\frac{\mathrm{d}\underline{\mathbf{m}}}{\mathrm{d}t}\right|^2 = -\sum_{l=1}^{N}\alpha\left|\frac{\mathrm{d}\mathbf{m}_l}{\mathrm{d}t}\right|^2, \tag{35}$$

finally, in the case $\alpha = 0$, the semi-discretized LLG (29) takes the form

$$\frac{\mathrm{d}\underline{\mathbf{m}}}{\mathrm{d}t} = \underline{\Lambda}(\underline{\mathbf{m}})\cdot\frac{\partial g}{\partial\underline{\mathbf{m}}}, \tag{36}$$

which is related to the semi-discretized version of Poisson bracket (22)

$$\{f(\underline{\mathbf{m}}), h(\underline{\mathbf{m}})\} = \frac{\partial f}{\partial\underline{\mathbf{m}}}\cdot\underline{\Lambda}(\underline{\mathbf{m}})\cdot\frac{\partial h}{\partial\underline{\mathbf{m}}}, \tag{37}$$

where $f(\underline{\mathbf{m}})$ and $h(\underline{\mathbf{m}})$ are two generic functions of $\underline{\mathbf{m}}$, and $\partial f/\partial\underline{\mathbf{m}}$, $\partial h/\partial\underline{\mathbf{m}}$ are the corresponding gradients.

In connection with the hamiltonian structure (36), it is interesting to mention that, when the matrix $\underline{\Lambda}(\underline{\mathbf{m}})$ has the linear form (31), the related hamiltonian system (36) is said to have a Lie–Poisson structure [25]. As we will discuss in the sequel, this structure affects the nature of mid-point approximation of LLG equation.

4. Qualitative properties of mid-point LLG discrete dynamics

We now proceed to derive the full discretization of LLG equation by applying the mid-point rule to the spatially semi-discretized system of ODEs given by Eq. (28). In the following, we will denote the value of physical quantities at the nth time-step with the suffix n. The mid-point rule consists in the following time-stepping scheme, written for the generic lth cell:

$$\frac{\mathbf{m}_l^{n+1}-\mathbf{m}_l^n}{\Delta t} = -\left(\frac{\mathbf{m}_l^{n+1}+\mathbf{m}_l^n}{2}\right)\times\left[\mathbf{h}_{\mathrm{eff},l}\left(\frac{\underline{\mathbf{m}}^{n+1}+\underline{\mathbf{m}}^n}{2}, t^n+\frac{\Delta t}{2}\right)-\alpha\frac{\mathbf{m}_l^{n+1}-\mathbf{m}_l^n}{\Delta t}\right], \tag{38}$$

where Δt is the time-step, which, for the sake of simplicity, is assumed here constant. Nevertheless, due to the single-step nature of mid-point rule, most considerations in the following can be generalized to non-constant time-steps. Eq. (38) can be rewritten in terms of mesh vectors as follows:

$$\frac{\underline{\mathbf{m}}^{n+1}-\underline{\mathbf{m}}^n}{\Delta t} = -\underline{\Lambda}\left(\frac{\underline{\mathbf{m}}^{n+1}+\underline{\mathbf{m}}^n}{2}\right)\cdot\left[\underline{\mathbf{h}}_{\mathrm{eff}}\left(\frac{\underline{\mathbf{m}}^{n+1}+\underline{\mathbf{m}}^n}{2}, t^n+\frac{\Delta t}{2}\right)-\alpha\frac{\underline{\mathbf{m}}^{n+1}-\underline{\mathbf{m}}^n}{\Delta t}\right]. \tag{39}$$

Eq. (39) defines $\underline{\mathbf{m}}^{n+1}$ in terms of $\underline{\mathbf{m}}^n$ implicitly. By solving this equation for $\underline{\mathbf{m}}^{n+1}$, we generate a map

$$\underline{\mathbf{m}}^{n+1} = \Phi^n(\Delta t, \underline{\mathbf{m}}^n), \tag{40}$$

which describes the LLG discrete dynamics. We will discuss the technique for solving the implicit Eq. (39) in the following section. In this section, we will focus on the properties of the map (40) defined implicitly by Eq. (38) or equivalently by Eq. (39).

As a preliminary consideration, we notice that, in most LLG numerical investigations, the discretization of LLG equation is carried out starting from the Landau–Lifshitz form (7), which has the advantage of explicitly expressing the time derivative of $\mathbf{m}$. Conversely, in the approach we propose, we directly discretize the original LLG equation in which the time derivative is implicitly contained. In fact, since the mid-point scheme is already implicit, the implicit nature of LLG equation does not introduce any further complication, but rather it drastically simplifies the treatment of damping in the algorithm.

The first important property of the discrete dynamics can be readily obtained from Eq. (38) by scalar multiplying both sides of the equation by $(\mathbf{m}_l^{n+1}+\mathbf{m}_l^n)$. This leads immediately to

$$(\mathbf{m}_l^{n+1} - \mathbf{m}_l^n) \cdot (\mathbf{m}_l^{n+1} + \mathbf{m}_l^n) = |\mathbf{m}_l^{n+1}|^2 - |\mathbf{m}_l^n|^2 = 0, \quad l = 1, \ldots, N, \tag{41}$$

which means that the magnitude of the magnetization vector remains constant in each cell. Thus, the mid-point rule preserves exactly the property (33), regardless of the time-step.

Next, we analyze the energy balance properties of the discrete dynamics. The derivation of the main equation can be carried out by scalar multiplying both sides of Eq. (39) by the quantity

$$\left[\underline{\mathbf{h}}_{\text{eff}}\left(\frac{\underline{\mathbf{m}}^{n+1} + \underline{\mathbf{m}}^n}{2}, t^n + \frac{\Delta t}{2}\right) - \alpha\frac{\underline{\mathbf{m}}^{n+1} - \underline{\mathbf{m}}^n}{\Delta t}\right]. \tag{42}$$

It is clear that, due to the antisymmetry of the matrix $\underline{\Lambda}(\underline{\mathbf{m}})$ (which is related to the antisymmetry of its 3×3 diagonal blocks), the dot multiplication of (42) and the right-hand side of Eq. (39) gives zero. As far as the left-hand side is concerned, by using the expression of the discretized effective field (26), one obtains

$$\frac{\underline{\mathbf{m}}^{n+1} - \underline{\mathbf{m}}^n}{\Delta t} \cdot \left[-\underline{C} \cdot \left(\frac{\underline{\mathbf{m}}^{n+1} + \underline{\mathbf{m}}^n}{2}\right) + \underline{\mathbf{h}}_{\text{a}}\left(t^n + \frac{\Delta t}{2}\right) - \alpha\frac{\underline{\mathbf{m}}^{n+1} - \underline{\mathbf{m}}^n}{\Delta t}\right] = \mathbf{0}. \tag{43}$$

Then, we use the following mid-point approximation for $\underline{\mathbf{h}}_{\text{a}}$:

$$\underline{\mathbf{h}}_{\text{a}}\left(t^n + \frac{\Delta t}{2}\right) = \frac{\underline{\mathbf{h}}_{\text{a}}^{n+1} + \underline{\mathbf{h}}_{\text{a}}^n}{2} - \frac{\Delta t^2}{4}\frac{\mathrm{d}^2\underline{\mathbf{h}}_{\text{a}}}{\mathrm{d}t^2}\bigg|_{t^n + \frac{\Delta t}{2}} + \underline{\mathbf{R}}_{\text{a}}(t^n, \Delta t), \tag{44}$$

where $\underline{\mathbf{R}}_{\text{a}}(t^n, \Delta t)$ is the remainder of the mid-point formula which is infinitesimal of order 4 with respect to Δt. Now, by taking into account the symmetry of the matrix $\underline{C}$ and Eq. (44) one can readily derive the following equation:

$$\begin{aligned}\frac{\underline{g}(\underline{\mathbf{m}}^{n+1}; \underline{\mathbf{h}}_{\text{a}}^{n+1}) - \underline{g}(\underline{\mathbf{m}}^n; \underline{\mathbf{h}}_{\text{a}}^n)}{\Delta t} = & -\alpha\left|\frac{\underline{\mathbf{m}}^{n+1} - \underline{\mathbf{m}}^n}{\Delta t}\right|^2 - \frac{(\underline{\mathbf{m}}^{n+1} + \underline{\mathbf{m}}^n)}{2} \cdot \frac{\underline{\mathbf{h}}_{\text{a}}^{n+1} - \underline{\mathbf{h}}_{\text{a}}^n}{\Delta t} \\ & - \frac{\Delta t^2}{4}\frac{\mathrm{d}^2\underline{\mathbf{h}}_{\text{a}}}{\mathrm{d}t^2}\bigg|_{t^n + \frac{\Delta t}{2}} \cdot \frac{(\underline{\mathbf{m}}^{n+1} - \underline{\mathbf{m}}^n)}{\Delta t} + \underline{\mathbf{R}}_{\text{a}}(t^n, \Delta t) \cdot \frac{(\underline{\mathbf{m}}^{n+1} - \underline{\mathbf{m}}^n)}{\Delta t}.\end{aligned} \tag{45}$$

This equation shows that the discrete dynamics reproduces the energy balance for semi-discretized equation (34) up to second order terms in Δt.

We preliminarily notice that, when the applied field $\underline{\mathbf{h}}_{\text{a}}$ is piece-wise linear function of time in each interval $[t^n, t^{n+1}]$, the last two terms in the right-hand side vanish and the energy balance is exactly reproduced in its mid-point time discretized version.

More importantly, in the case of constant applied field, the last three terms in right-hand side of Eq. (45) vanish and the energy balance reduces to the following form:

$$\frac{\underline{g}(\underline{\mathbf{m}}^{n+1}; \underline{\mathbf{h}}_{\text{a}}) - \underline{g}(\underline{\mathbf{m}}^n; \underline{\mathbf{h}}_{\text{a}})}{\Delta t} = -\alpha\left|\frac{\underline{\mathbf{m}}^{n+1} - \underline{\mathbf{m}}^n}{\Delta t}\right|^2. \tag{46}$$

Eq. (46) has very important consequences. First, independently of the time-step, the discretized energy $\underline{g}(\underline{\mathbf{m}}^n; \underline{\mathbf{h}}_{\text{a}})$ is decreasing. This confirms that the mid-point rule is an unconditionally stable algorithm which reproduces the relaxation behavior in LLG discrete dynamics for any choice of the time-step. Notice also that the rate of change of energy in the discrete dynamics is coherent the mid-point version of Eq. (35).

Second, for $\alpha = 0$ the energy is exactly preserved regardless of the time-steps. These two properties confirm the unconditional stability of mid-point rule, but more importantly they indicate that, in the short time scale, the mid-point rule will tend to reproduce correctly the most important part in the LLG dynamics, i.e. the precessional magnetization motion.

Finally, it is also important to address the issue of the preservation of hamiltonian structure [12] (in the case $\alpha = 0$) given by Eq. (36). Let us indicate by $\underline{\mathbf{m}}(t) = \phi(t, \underline{\mathbf{m}}_0)$ the flow of Eq. (36), namely the solution of

the Cauchy problem for the system of ODEs (36) with the initial condition $\underline{\mathbf{m}}(t = t_0) = \underline{\mathbf{m}}_0$. It is well known [25] that the map $\phi(t, \underline{\mathbf{m}}_0)$, mapping $\underline{\mathbf{m}}_0$ into $\underline{\mathbf{m}}(t)$, satisfies the following symplecticity condition:

$$\frac{\partial \phi(t, \underline{\mathbf{m}}_0)}{\partial \underline{\mathbf{m}}_0} \cdot \underline{\Lambda}(\underline{\mathbf{m}}_0) \cdot \left(\frac{\partial \phi(t, \underline{\mathbf{m}}_0)}{\partial \underline{\mathbf{m}}_0} \right)^{\mathrm{T}} = \underline{\Lambda}(\phi(t, \underline{\mathbf{m}}_0)). \tag{47}$$

A numerical scheme is said to preserve the hamiltonian structure if the associated map, which connects one step to the following (in the case of mid-point rule the map $\Phi^n(\Delta t, \underline{\mathbf{m}}^n)$ introduced in Eq. (40)), fulfills the condition (47). In this respect, by using the fact that the LLG equation has a Lie–Poisson structure (i.e. the matrix $\underline{\Lambda}(\underline{\mathbf{m}})$ is linear with respect to $\underline{\mathbf{m}}$ as expressed in Eq. (31)), it is possible to prove the following error formula [3]:

$$\frac{\partial \Phi^n(\Delta t, \underline{\mathbf{m}}^n)}{\partial \underline{\mathbf{m}}^n} \cdot \underline{\Lambda}(\underline{\mathbf{m}}^n) \cdot \left(\frac{\partial \Phi^n(\Delta t, \underline{\mathbf{m}}^n)}{\partial \underline{\mathbf{m}}^n} \right)^{\mathrm{T}} - \underline{\Lambda}(\Phi^n(\Delta t, \underline{\mathbf{m}}^n)) = \mathcal{O}(\Delta t^3), \tag{48}$$

where $\mathcal{O}(\Delta t^n)$ indicates an infinitesimal of order n. Eq. (48) implies that the mid-point rule applied to LLG equation preserves hamiltonian structure up to the third order term in Δt.

It is also interesting to notice that the preservation of hamiltonian structure would be exact for an hamiltonian system defined by a Poisson bracket of the type $\{f(\underline{\mathbf{m}}), h(\underline{\mathbf{m}})\} = \partial f/\partial \underline{\mathbf{m}} \cdot \underline{J} \cdot \partial h/\partial \underline{\mathbf{m}}$, where the matrix $\underline{J}$ does not depend on $\underline{\mathbf{m}}$ [11]. In magnetization dynamics studies this situation is encountered in all those problems in which LLG equation is linearized around a given magnetization state as it is generally done in spin-wave analysis and nucleation problems [1]. In this respect, it must be underlined that, although these problems are linear in nature, analytical solutions are obtainable only under quite restrictive assumptions about the geometry of the magnetic body. General geometries can be treated only by numerical techniques.

5. Solution of the time-stepping equation

The properties we have just discussed are strongly related to the implicit nature of mid-point rule. As a consequence of this implicit nature, we have to solve the time-stepping equation (39) for the unknown $\underline{\mathbf{m}}^{n+1}$ at each time-step which amounts to solve the following system of $3N$ nonlinear equations in the $3N$ unknowns $\underline{\mathbf{m}}^{n+1}$:

$$\mathbf{F}^n(\underline{\mathbf{m}}^{n+1}) = \mathbf{0}, \tag{49}$$

where $\mathbf{F}^n(\underline{\mathbf{y}}) : \mathbb{R}^{3N} \to \mathbb{R}^{3N}$ is the following vector function:

$$\mathbf{F}^n(\underline{\mathbf{y}}) = \left[\underline{\mathbf{I}} - \alpha \underline{\Lambda} \left(\frac{\underline{\mathbf{y}} + \underline{\mathbf{m}}^n}{2} \right) \right] \cdot \left(\underline{\mathbf{y}} - \underline{\mathbf{m}}^n \right) - \Delta t \, \mathbf{f}^n \left(\frac{\underline{\mathbf{y}} + \underline{\mathbf{m}}^n}{2} \right), \tag{50}$$

and where

$$\mathbf{f}^n(\underline{\mathbf{m}}) = -\underline{\Lambda}(\underline{\mathbf{m}}) \cdot \underline{\mathbf{h}}_{\mathrm{eff}} \left(\underline{\mathbf{m}}, t^n + \frac{\Delta t}{2} \right) = \underline{\Lambda}(\underline{\mathbf{m}}) \cdot \frac{\partial g}{\partial \underline{\mathbf{m}}} \left(\underline{\mathbf{m}}; \underline{\mathbf{h}}_{\mathrm{a}} \left(t^n + \frac{\Delta t}{2} \right) \right) \tag{51}$$

is the right-hand side of the conservative semi-discretized LLG Equation (29).

The solution of the system of equations (49) can be obtained by using Newton–Raphson (NR) algorithm. To this end, we derive the jacobian matrix $\underline{J}_F^n(\underline{\mathbf{y}})$ of the vector function $\mathbf{F}^n(\underline{\mathbf{y}})$, which, after simple algebraic manipulations, can be written in the following form:

$$\underline{J}_F^n(\underline{\mathbf{y}}) = \underline{\mathbf{I}} - \alpha \underline{\Lambda}(\underline{\mathbf{m}}^n) - \frac{\Delta t}{2} \underline{J}_f^n \left(\frac{\underline{\mathbf{y}} + \underline{\mathbf{m}}^n}{2} \right), \tag{52}$$

where $\underline{J}_f^n$ is the jacobian matrix associated to $\mathbf{f}^n(\underline{\mathbf{m}})$. By using Eqs. (31) and (51), one obtains

$$\underline{J}_f^n(\underline{\mathbf{m}}) = \frac{\partial \mathbf{f}^n}{\partial \underline{\mathbf{m}}}(\underline{\mathbf{m}}) = \underline{\Lambda}(\underline{\mathbf{m}}) \cdot \underline{C} + \underline{\Gamma} \cdot \left[-\underline{C} \cdot \underline{\mathbf{m}} + \underline{\mathbf{h}}_a\left(t^n + \frac{\Delta t}{2}\right)\right]. \tag{53}$$

The main difficulty in applying NR method is that the Jacobian $\underline{J}_F^n(\underline{\mathbf{y}})$ of $\mathbf{F}^n(\underline{\mathbf{y}})$ is a full matrix, due to the long-range character of magnetostatic interactions. In this connection, let us observe that the damping term affects only a (small for $\alpha \ll 1$) sparse component of the jacobian $\underline{J}_F^n(\underline{\mathbf{y}})$ and thus does not introduce any additional difficulty.

It is important to stress that, due to the full nature of $\underline{J}_F^n(\underline{\mathbf{y}})$, the use of the plain NR method would require an unpractical computational cost. This problem can be circumvented, as it is usual in solving field problems with implicit time-stepping [35], by using a quasi-Newton method. This consists in considering a reasonable and sparse approximation of the Jacobian. In this respect, we consider the following expression $\tilde{\underline{J}}_F^n$ in which magnetostatic interactions are not included:

$$\tilde{\underline{J}}_F^n(\underline{\mathbf{y}}) = \underline{\mathbf{I}} - \alpha \underline{\Lambda}(\underline{\mathbf{m}}^n) - \frac{\Delta t}{2}\tilde{\underline{J}}_f^n\left(\frac{\underline{\mathbf{y}} + \underline{\mathbf{m}}^n}{2}\right), \tag{54}$$

where the matrix $\tilde{\underline{J}}_f^n$ is

$$\tilde{\underline{J}}_f^n(\underline{\mathbf{m}}) = -\underline{\Lambda}(\underline{\mathbf{m}}) \cdot (-(\underline{C}_{ex} + \underline{C}_{an})) + \underline{\Gamma} \cdot \left[-(\underline{C}_{ex} + \underline{C}_{an}) \cdot \underline{\mathbf{m}} + \underline{\mathbf{h}}_a\left(t^n + \frac{\Delta t}{2}\right)\right]. \tag{55}$$

Basically, the latter equation is obtained by substituting in Eq. (53) the full matrix $\underline{C}$ with its sparse component $\underline{C}_{ex} + \underline{C}_{an}$. Thus, the iterative procedure can be summarized as follows:

$$\underline{\mathbf{y}}_0 = \underline{\mathbf{m}}^n, \quad \underline{\mathbf{y}}_{k+1} = \underline{\mathbf{y}}_k + \Delta \underline{\mathbf{y}}_{k+1} \qquad \text{with } \tilde{\underline{J}}_F^n(\underline{\mathbf{y}}_k)\Delta \underline{\mathbf{y}}_{k+1} = -\mathbf{F}^n(\underline{\mathbf{y}}_k). \tag{56}$$

At each iteration, the linear system defined by the matrix (55) has to be inverted. Since this matrix is non-symmetric, we have found appropriate to use generalized minimum residual (GMRES) method [32]. The iteration (56) is repeated until the norm $\|\mathbf{F}^n(\underline{\mathbf{y}}_k)\|$ is under a prescribed tolerance.

The iterative technique we developed to solve Eq. (49) belongs to the category of quasi-Newton methods. It has been proven that this kind of iterative procedures is convergent provided that the initial guess is sufficiently close to the 'true' solution of the system and the order of convergence is the first order [29]. In this respect, we have relied on the continuation of the numerical solution: the initial guess for the solution at the time-step $n + 1$ is the magnetization state $\underline{\mathbf{m}}^n$.

It is interesting to notice that, if one considers a model in which the demagnetizing field is neglected, the iterative procedure (56) becomes a pure Newton–Raphson algorithm with quadratic convergence [29]. This kind of model is generally used to analyze ferromagnetic bodies in such small spatial scale that the exchange and anisotropy interactions are the only relevant interactions [23]. Another area where one is interested in LLG-like equation without demagnetizing field is the study of integrable spin models and Heisenberg model [13].

6. Accuracy and stability tests for LLG discrete dynamics

We have shown that mid-point rule time-stepping preserves magnetization magnitude and Lyapunov structure of LLG equation. Nevertheless, since the time-stepping equations (39) are solved through an iterative procedure, the properties of mid-point rule we have discussed in Section 4 are fulfilled only within a certain accuracy related to the tolerance which we impose on the quasi-NR technique. In this respect, it is important to test the accuracy of the preservation of LLG properties during the computation.

To this end, as far as magnetization magnitude conservation is concerned, we will check the accuracy with the following quantities:

$$m_{\mathrm{av}} = \frac{1}{N}\sum_{l=1}^{N} |\mathbf{m}_l|, \quad \sigma_{\mathrm{m}}^2 = \frac{1}{N}\sum_{l=1}^{N} (|\mathbf{m}_l| - m_{\mathrm{av}})^2, \tag{57}$$

which are, respectively, mean value and variance of the magnetization magnitude over the cells of the mesh.

Let us observe that since the conservation of magnetization amplitude is usually controlled either with geometric integration or renormalization at each time-step, numerical instabilities will not manifest themselves through the divergence of $\underline{\mathbf{m}}$, but with anomalous behavior of energy.

Thus, as far as the energy balance equation is concerned, we use the self-consistency criterion proposed by Albuquerque and coworkers [2]. This criterion is valid for constant applied field and is based on Eq. (35) rewritten in the following form:

$$\alpha = \left(\frac{\mathrm{d}}{\mathrm{d}t}\underline{g}(\underline{\mathbf{m}}(t);\underline{\mathbf{h}}_{\mathrm{a}})\right) \Bigg/ \left|\frac{\mathrm{d}\underline{\mathbf{m}}}{\mathrm{d}t}\right|^2. \tag{58}$$

To test the preservation of energy dynamics in numerical computation, we consider the value

$$\hat{\alpha}^n = -\left(\frac{\underline{g}(\underline{\mathbf{m}}^{n+1};\underline{\mathbf{h}}_{\mathrm{a}}) - \underline{g}(\underline{\mathbf{m}}^{n};\underline{\mathbf{h}}_{\mathrm{a}})}{\Delta t}\right) \Bigg/ \left|\frac{\underline{\mathbf{m}}^{n+1} - \underline{\mathbf{m}}^{n}}{\Delta t}\right|^2, \tag{59}$$

computed at each time-step, and we compare it with the constant α. We observe that if we could exactly invert the system of nonlinear equations (49), according to property expressed in Eq. (46), then the sequence $\hat{\alpha}^n$ would be constant and coincident with α. However, since we determine $\underline{\mathbf{m}}^{n+1}$ by an iterative procedure the sequence will be in fact nonconstant and it will usually exhibit an oscillatory behavior. In particular, unstable behaviors correspond to negative $\hat{\alpha}^n$.

For the case of conservative dynamics, the discretized energy is conserved according to Eq. (35) (for $\alpha = 0$):

$$\underline{g}(\underline{\mathbf{m}}(t);\underline{\mathbf{h}}_{\mathrm{a}}) = \underline{g}(\underline{\mathbf{m}}(t_0);\underline{\mathbf{h}}_{\mathrm{a}}) \quad \forall t \geqslant t_0. \tag{60}$$

After mid-point rule time discretization, this property becomes (see Eq. (46)):

$$\underline{g}(\underline{\mathbf{m}}^{n+1};\underline{\mathbf{h}}_{\mathrm{a}}) = \underline{g}(\underline{\mathbf{m}}^{n};\underline{\mathbf{h}}_{\mathrm{a}}), \tag{61}$$

which holds regardless of the time-step. One can test the accuracy of the scheme by recording the deviation of the total energy from its initial value. Again, one cannot expect that this property will be exactly fulfilled since we solve the time-stepping algorithm with an iterative procedure. In this respect, we will verify a posteriori that the energy conservation is guaranteed with sufficient precision by computing the relative error e_{g} of $\underline{g}(\underline{\mathbf{m}}^{n};\underline{\mathbf{h}}_{\mathrm{a}})$ with respect to the initial energy $\underline{g}(\underline{\mathbf{m}}^{0};\underline{\mathbf{h}}_{\mathrm{a}})$:

$$e_{\mathrm{g}}^n = \frac{\underline{g}(\underline{\mathbf{m}}^{n};\underline{\mathbf{h}}_{\mathrm{a}}) - \underline{g}(\underline{\mathbf{m}}^{0};\underline{\mathbf{h}}_{\mathrm{a}})}{\underline{g}(\underline{\mathbf{m}}^{0};\underline{\mathbf{h}}_{\mathrm{a}})}, \tag{62}$$

and checking that the sequence e_{g}^n remains within prescribed tolerance.

7. Finite difference spatial discretization of LLG equation

Up to this point the considerations we made about the properties and the implementation of mid-point rule were rather independent from the spatial discretization used. In the following, to test the method we have chosen a specific technique based on finite difference method. The magnetic body is subdivided into a

collection of rectangular prisms with edges parallel to the coordinate axes. The edge lengths are d_x, d_y, d_z. In this framework, it is convenient to identify each cell by three indices i, j, k instead of using the index l as we did before. The magnetization $\mathbf{m}_{i,j,k}$ is assumed to be uniform within the generic (i, j, k) cell. With this notation, the effective field in the generic (i, j, k) cell can be expressed as

$$\mathbf{h}_{\mathrm{eff};i,j,k} = \mathbf{h}_{\mathrm{ex};i,j,k} + \mathbf{h}_{\mathrm{m};i,j,k} + \mathbf{h}_{\mathrm{an};i,j,k} + \mathbf{h}_{\mathrm{a};i,j,k}. \tag{63}$$

The exchange field $\mathbf{h}_{\mathrm{ex};i,j,k}$ is computed by means of a 7-point laplacian discretization, which is second order accurate in space. In the generic "internal" cell (i, j, k), it can be expressed as follows:

$$\mathbf{h}_{\mathrm{ex};i,j,k} = \frac{2A}{\mu_0 M_{\mathrm{s}}^2}\left[\frac{\mathbf{m}_{i+1,j,k}+\mathbf{m}_{i-1,j,k}}{d_y^2} + \frac{\mathbf{m}_{i,j+1,k}+\mathbf{m}_{i,j-1,k}}{d_x^2} + \frac{\mathbf{m}_{i,j,k+1}+\mathbf{m}_{i,j,k-1}}{d_z^2} - \left(\frac{2}{d_y^2}+\frac{2}{d_x^2}+\frac{2}{d_z^2}\right)\mathbf{m}_{i,j,k}\right]. \tag{64}$$

A similar expression holds for the boundary cells, where the Neumann boundary condition (11) has to be taken into account. Since the exchange interaction is a first-neighbors interaction, one can easily observe that the matrix $\underline{C}_{\mathrm{ex}}$ is a block-diagonal matrix.

The magnetostatic field $\mathbf{h}_{\mathrm{m};i,j,k}$ can be expressed as discrete convolution [34,45]:

$$\mathbf{h}_{m;i,j,k} = \sum_{i'\neq i}\sum_{j'\neq j}\sum_{k'\neq k} N_{i-i',j-j',k-k'} \cdot \mathbf{m}_{i',j',k'} d_x d_y d_z, \tag{65}$$

where $N_{i-i',j-j',k-k'}$ is the 3×3 block of the magnetostatic interaction matrix $\underline{C}_{\mathrm{m}}$ which describes the magnetostatic interaction between the cells i, j, k and i', j', k'. The discrete convolution (65) is computed by means of 3D Fast Fourier Transform (FFT) using the zero-padding algorithm [5]. The kernel of the convolution is obtained by means of a generalization to prism (non cubic) cells of the formulas proposed in [34] for cubic cells. As far as anisotropy is concerned, we assume that the anisotropy field is

$$\mathbf{h}_{\mathrm{an};i,j,k} = \frac{2K_1}{\mu_0 M_{\mathrm{s}}^2}(\mathbf{m}_{i,j,k}\cdot\mathbf{e}_{\mathrm{an}})\mathbf{e}_{\mathrm{an}}. \tag{66}$$

and the matrix $\underline{C}_{\mathrm{an}}$ is a diagonal matrix.

8. Numerical simulations of μ-mag standard problem no. 4

We have applied the above numerical technique to solve the μ-mag standard problem no. 4 (see [28]). This problem concerns the study of magnetization reversal dynamics in a permalloy thin-film subject to a constant and spatially uniform external field, applied almost antiparallel to the initial magnetization. The geometry of the medium is sketched in Fig. 1(a). The material parameters are $A = 1.3\times 10^{-11}$ J/m, $M_s = 8.0\times 10^5$ A/m, $K_1 = 0$ J/m^3 and $\alpha = 0.02$. The initial state is an equilibrium "S-state" (see [28] and Fig. 1(b)) such as is obtained after applying and slowly reducing a saturating field along the [1, 1, 1] direction to zero [28]. In all the numerical simulations, the magnetization is assumed to have reached equilibrium when

$$\max_{l=1,\ldots,N}\left|\frac{\mathbf{m}_l^{n+1}-\mathbf{m}_l^n}{\Delta t}\right| < \varepsilon_{\mathrm{torque}}, \tag{67}$$

i.e. the maximum of the (normalized) torque across the body is less than a prescribed tolerance $\varepsilon_{\mathrm{torque}}$. For our computations we have chosen $\varepsilon_{\mathrm{torque}} = 10^{-5}$. Moreover, the stopping criterion of the quasi-Newton iterative procedure has been chosen

$$\max_{q=1,\ldots,3N}|F_q^n(\underline{\mathbf{y}}_k)| < 10^{-14}, \tag{68}$$

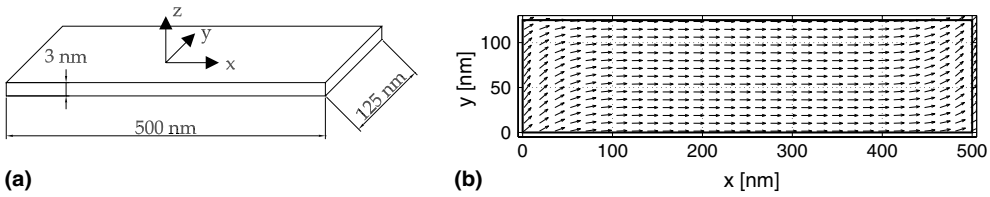

Fig. 1. (a) Thin-film geometry for μ-mag standard problem no. 4; (b) initial equilibrium S-state.

where $F_q^n(\underline{\mathbf{y}}_k)$ is the qth component of the vector $\mathbf{F}^n(\underline{\mathbf{y}}_k)$, and the index k indicates the number of quasi-Newton iterations.

Two switching events have been calculated using fields applied in the x–y plane of different magnitude and direction. In the first case the external field is applied at an angle of 170° off the x axis with x–y components such that $\mu_0 M_s h_{ax} = -24.6$ mT, $\mu_0 M_s h_{ay} = 4.3$ mT and $\mu_0 h_a = 25$ mT. In the second case the external field is applied at an angle of 190° off the x axis with x–y components such that $\mu_0 M_s h_{ax} = -35.5$ mT, $\mu_0 M_s h_{ay} = -6.3$ mT, and $\mu_0\ M_s h_a = 36$ mT. In both cases the cell edges are $d_x = 3.125$ nm, $d_y = 3.125$ nm, $d_z = 3$ nm and therefore the number of cells is $N = 160 \times 40 \times 1 = 6400$.

Next we report the comparison between the solution obtained using the above numerical technique and the solutions submitted by other researchers [28] to the μ-mag website. The time-step of the mid-point numerical algorithm is constant and it is such that $(\gamma M_s)^{-1}\Delta t = 2.5$ ps. This value has been chosen only on the basis of accuracy, since the mid-point rule is unconditionally stable. In this respect, we observe that the time-steps chosen in the other submitted computations (see [28]) are considerably smaller (from tens of femtoseconds to 0.2 picoseconds). These small time-steps are presumably due to numerical stability requirements.

In the results presented in the sequel, we plot average value of magnetization components. For instance, the average value $\langle m_x \rangle$ of the m_x component is computed as

$$\langle m_x \rangle = \frac{1}{N} \sum_{i,j,k} m_{x;i,j,k}. \tag{69}$$

In Figs. 2 and 3 plots of $\langle m_y \rangle$ as a function of time are reported. We observe that in the first case (Fig. 2) there is substantial agreement between the submitted solutions (see [28]) and for this reason we report, for comparison purposes, only the solution proposed by McMichael and coworkers. In Fig. 4 the plots of magnetization vector field when $\langle m_x \rangle$ crosses zero for the first time are reported. To check whether the numerical solution depends on the cells size, numerical simulations of the same problem were performed with a smaller cell edge (2.5 nm, number of cells $N = 10000$). The results reported in Fig. 5 show that the magnetization dynamics, computed for the two different mesh sizes, are almost coincident. As far as accuracy is concerned, the self-consistency conditions mentioned in Section 6 have been verified by means of the computation of the values m_{av}, σ_{m}^2 and $\hat{\alpha}^n$. The result of this computations is reported in Figs. 6 and 7. One can observe from Fig. 6 that the magnetization magnitude is very well preserved, since the mean value $m_{\mathrm{av}} \sim 1 \pm 10^{-16}$ and the variance σ_{m}^2 is in the order of 10^{-30}. It is remarkable that, despite the fact that we have not enforced the preservation of magnetization magnitude during the quasi-Newton iterations, the accuracy in magnetization magnitude conservation is within machine precision. In other words, there is numerical evidence that the stopping criterion expressed by Eq. (68) is somehow stronger than the preservation of magnetization magnitude.

Moreover, one can see from Fig. 7 that the relative error $e_\alpha^n = (\hat{\alpha}^n - \alpha)/\alpha$ is in the order of 10^{-7} in all cases. As far as conservative dynamics is concerned, the same problem has been simulated with $\alpha = 0$. The results, reported in Fig. 8, show that the reversal of the thin-film occurs, in the sense that the average

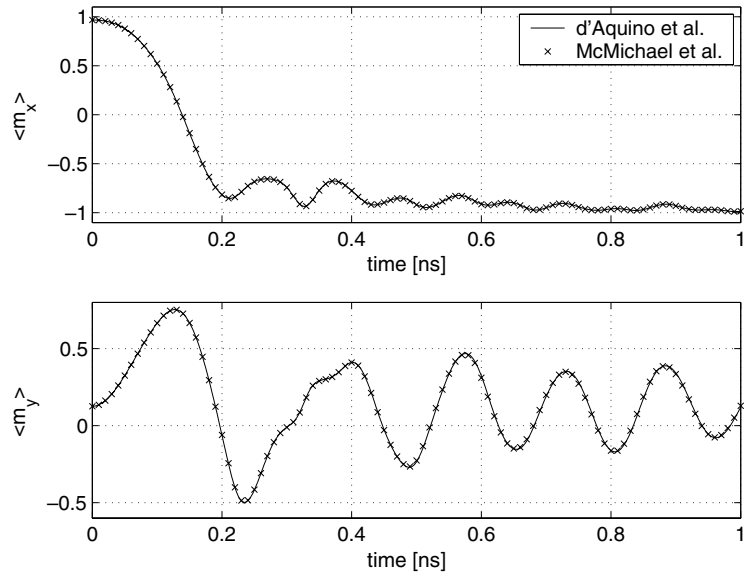

Fig. 2. Comparison between solutions of μ-mag standard problem no. 4. Plots of $\langle m_x \rangle$ and $\langle m_y \rangle$ versus time. The external field is applied at an angle of 170° off the x-axis.

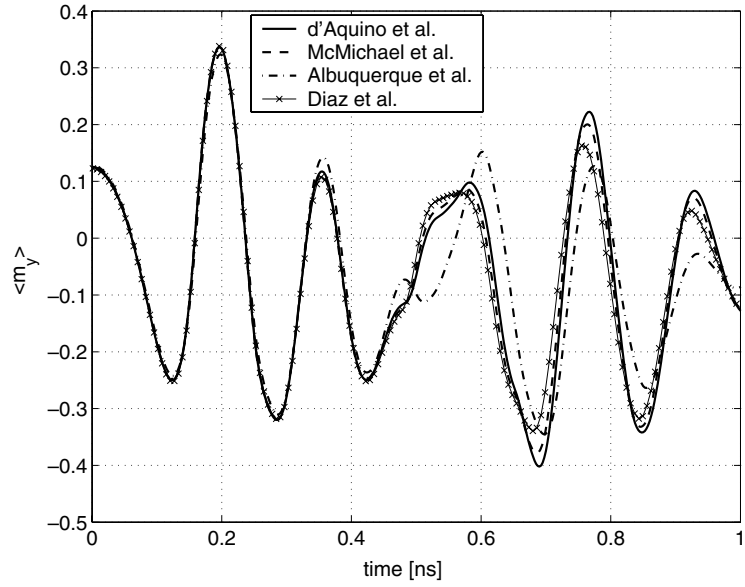

Fig. 3. Comparison between solutions of μ-mag standard problem no. 4. Plots of $\langle m_y \rangle$ versus time. The external field is applied at an angle of 190° off the x-axis.

magnetization exhibits a persistent oscillation around the reversed state. In fact, by comparing the magnetization behaviors for the conservative and dissipative case, reported in Fig. 9, one can observe that on a short time scale, in which the free energy is not so far from its initial value ($0 < t < 0.2$ ns), the conservative

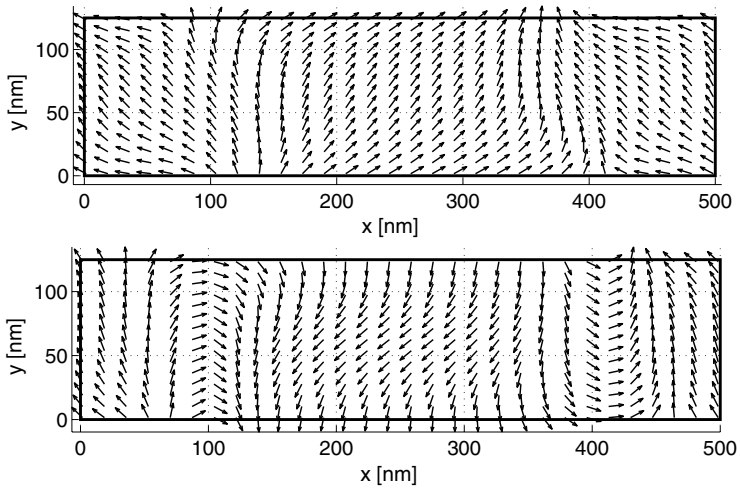

Fig. 4. Numerical results for μ-mag standard problem no. 4. Snapshot of magnetization vector field when the average $\langle m_x \rangle$ crosses zero for the first time. The external field is applied at an angle of 170° (up) and 190° (down) off the x-axis.

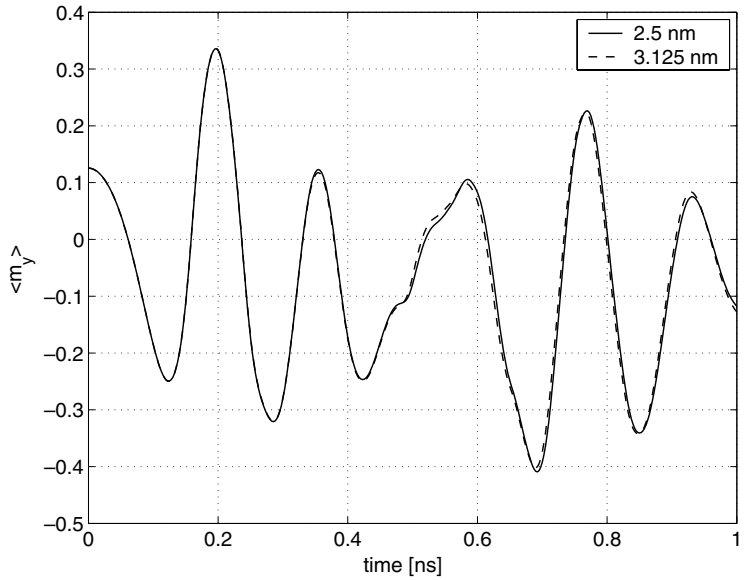

Fig. 5. Numerical results for μ-mag standard problem no. 4. Plots of $\langle m_y \rangle$ versus time for two different sizes of the mesh edge length. The external field is applied at an angle of 190° off the x-axis.

and dissipative dynamics are significantly close. This gives importance to the study of the conservative dynamics and means that the precessional effects are prevalent with respect to the damping effects in the reversal process. Let us stress that the free energy is conserved, as one can see from Fig. 10, where exchange, magnetostatic, anisotropy, Zeeman energy and the total free energy are reported as functions of time. In this experiment we have checked that the relative error e_g of the free energy with respect to its initial value is in the order of 10^{-8} as one can see from Fig. 11. We observe that the conservative switching process

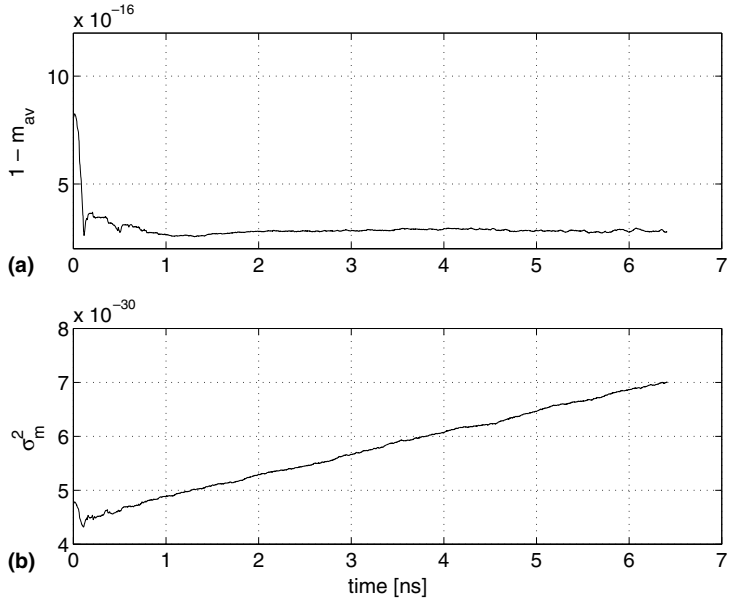

Fig. 6. Numerical results for μ-mag standard problem no. 4. (a) Plot of $1 - m_{\mathrm{av}}$ as a function of time. (b) Plot of the variance σ_{m}^2 as a function of time. In both plots $\delta = 190°$, $N = 6400$.

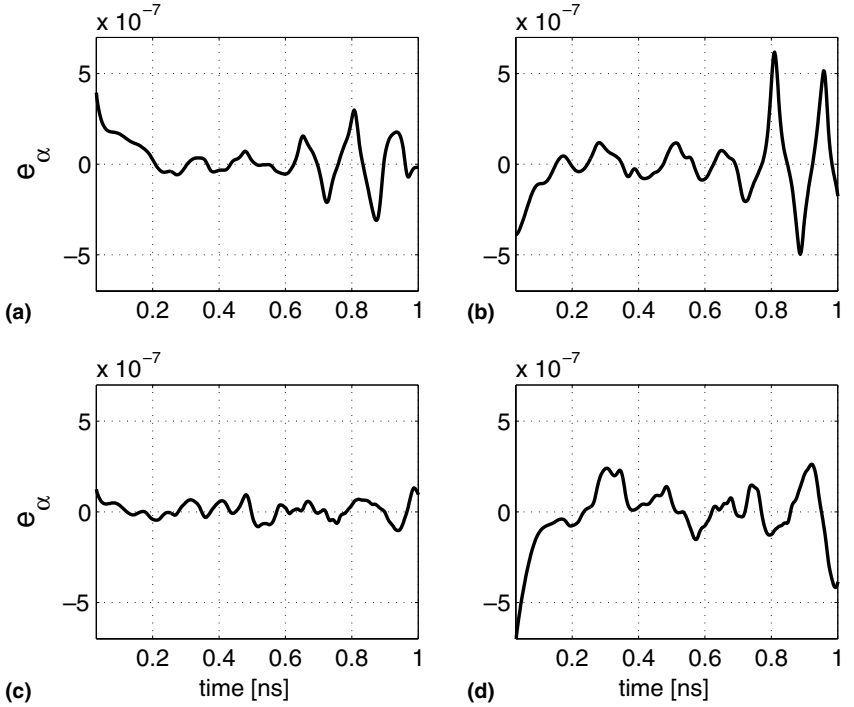

Fig. 7. Numerical results for μ-mag standard problem no. 4. Plot of the relative error $e_{\alpha}^{n} = (\hat{\alpha}^{n} - \alpha)/\alpha$ as a function of time. (a) $\delta = 170°$, $N = 6400$; (b) $\delta = 170°$, $N = 10000$; (c) $\delta = 190°$, $N = 6400$; (d) $\delta = 190°$, $N = 10000$.

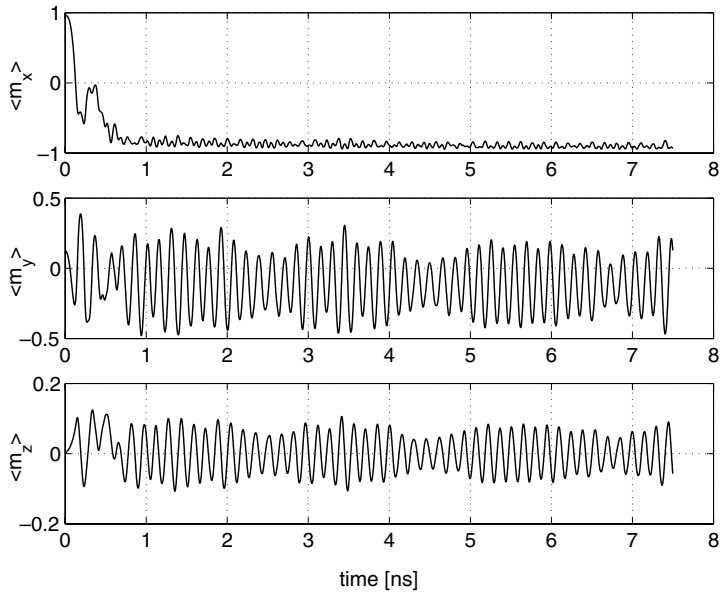

Fig. 8. Numerical results for μ-mag standard problem no. 4 in the conservative case $\alpha = 0$. Plot of $\langle m_x \rangle$ (top), $\langle m_y \rangle$ (middle), $\langle m_z \rangle$ (bottom) as functions of time. $\delta = 190°$, $N = 6400$.

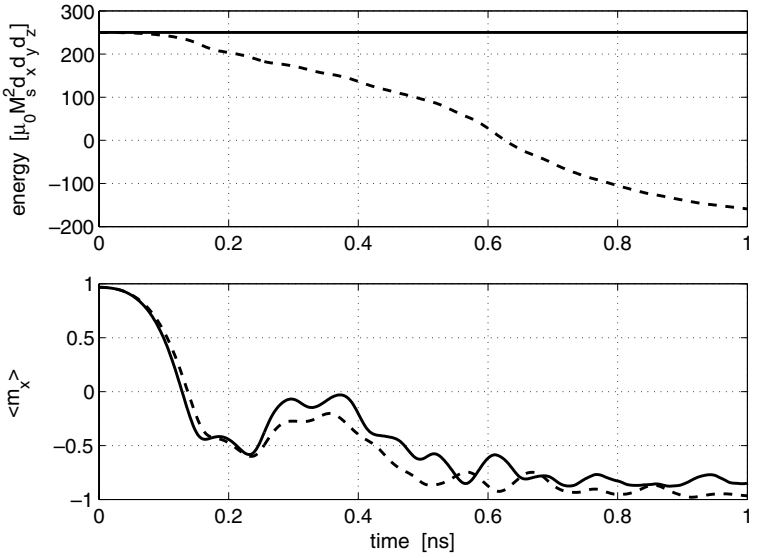

Fig. 9. Comparison of numerical results for μ-mag standard problem no. 4 in the conservative and dissipative case. Solid lines refer to the conservative case $\alpha = 0$, dashed lines refer to the dissipative case $\alpha = 0.02$. Plot of the free energy $\underline{g}$ (top), $\langle m_x \rangle$ (bottom) as functions of time. $\delta = 190°$, $N = 6400$.

occurs mainly through a transfer of energy from magnetostatic form to exchange form. This transfer of energy process is connected to the generation of spin-waves with decreasing wavelength [33].

As far as computational cost of our technique is concerned, numerical simulations for different number of cells and different time-steps have been performed besides the previous ones. As indicators, we have used

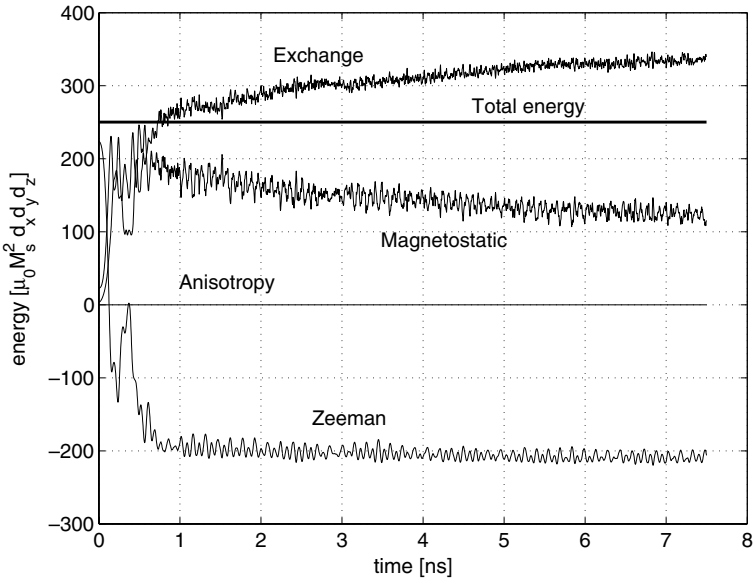

Fig. 10. Numerical results for μ-mag standard problem no. 4 in the conservative case $\alpha = 0$. Plot of exchange, anisotropy, magnetostatic, Zeeman and total free energy as functions of time. $\delta = 190°$, $N = 6400$.

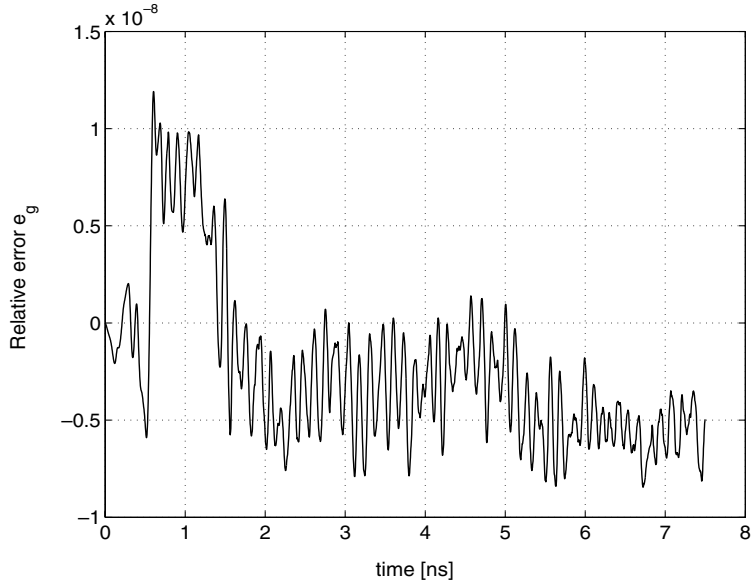

Fig. 11. Numerical results for μ-mag standard problem no. 4 in the conservative case $\alpha = 0$. Plot of the relative error $e_g^n = (\underline{g}(\underline{\mathbf{m}}^n; \underline{\mathbf{h}}_a) - \underline{g}(\underline{\mathbf{m}}^0; \underline{\mathbf{h}}_a))/\underline{g}(\underline{\mathbf{m}}^0; \underline{\mathbf{h}}_a)$ as function of time. $\delta = 190°$, $N = 6400$.

the average number of quasi-Newton iterations per time-step (NR), the average number of GMRES iterations in one quasi-Newton iteration (LIN), the simulated time T, the simulation time T_s and the ratio between them, the maximum relative error $e_{\alpha,\max} = \max|(\hat{\alpha}^n - \alpha)/\alpha|$, as functions of the orientation of the applied field δ, the number of cells N and the time-step. The results are summarized in Table 1. First,

Table 1
Numerical results

δ [deg]	N	$\frac{\Delta t}{\gamma M_s}$ [ps]	NR	LIN	$e_{\alpha,\max}$	T [ns]	T_s [s]	T_s/T [s/ns]
170	1000	2.5	11/14/17	4/5/5	1.5×10^{-8}	5.7700	648.05	112
170	2500	2.5	11/14/17	6/7/7	2.0×10^{-7}	5.8450	1976.47	338
170	6400	2.5	11/14/18	11/13/15	3.0×10^{-7}	5.8400	5631.23	964
170	10000	2.5	11/14/18	17/19/22	1.3×10^{-7}	5.8425	12152.74	2080
190	1000	2.5	11/14/17	4/5/5	1.4×10^{-8}	5.5800	632.34	113
190	2500	2.5	11/14/18	6/7/8	0.7×10^{-7}	6.4100	2183.36	341
190	6400	2.5	11/14/18	12/13/15	6.2×10^{-7}	6.4100	6257.13	976
190	10000	2.5	11/14/18	18/20/23	7.0×10^{-7}	6.4100	13546.79	2113
170	6400	1.0	9/12/14	6/6/7	3.7×10^{-7}	5.8420	10145.46	1737
170	6400	2.5	11/14/18	11/13/15	3.0×10^{-7}	5.8400	5631.23	964
170	6400	5.0	14/18/25	24/26/28	3.5×10^{-7}	5.9400	4624.31	779
190	6400	1.0	9/12/14	6/6/7	1.3×10^{-7}	6.4150	11163.490	1740
190	6400	2.5	11/14/18	12/13/15	6.2×10^{-7}	6.4100	6257.13	976
190	6400	5.0	14/18/27	23/26/30	1.1×10^{-7}	7.4950	5705.520	761

Indicators of computational cost for the proposed mid-point rule numerical technique. δ is the angle of the applied field, N is the number of cells, Δt is the time-step, column NR reports minimum/average/maximum number of quasi-Newton iterations per time-step, column LIN reports minimum/average/maximum number of GMRES iterations for one quasi-Newton iteration, $e_{\alpha,\max} = \max|(\hat{\alpha}^n - \alpha)/\alpha|$ is the maximum relative error with respect to the assigned damping parameter α, T is the simulated time, T_s the simulation time. $N = 1000$ refers to a prism cell of size $12.5\times5\times3$ nm. $N = 2500$ refers to a prism cell of size $5\times5\times3$ nm. $N = 6400$ refers to a prism cell of size $3.125\times3.125\times3$ nm. $N = 10000$ refers to a prism cell of size $2.5\times2.5\times3$ nm. The simulations have been performed with a Pentium 4 processor workstation (3 GHz), 1 GB RAM under RedHat Linux 9.

one can observe that the total number of cells N does not affect the number of quasi-Newton iterations in both the cases $\delta = 170°$ and $\delta = 190°$, whereas it affects the solution of the linear systems by increasing the average number of GMRES iterations. Second, one can clearly see that the minimum and maximum values of quasi-Newton and GMRES iterations are close to the average values, meaning that the iterative procedure weakly depends on magnetization dynamics and magnetization state, despite the approximate jacobian matrix $\underline{\tilde{J}}_F^n$ depends on the particular value of magnetization vector $\underline{\mathbf{m}}$. Third, some considerations on computational cost can be made. We expect that the computational cost function $C(N)$ of the algorithm, in terms of number of cells, can be reasonably expressed by the sum of two terms. In fact, at each quasi-Newton iteration the cost of the evaluation of magnetostatic field (3D FFT convolution [5]) is proportional to $N\log N$. On the other hand, in each quasi-Newton iteration, the cost of LIN iterations of GMRES is proportional to N, since basically is the cost of LIN sparse matrix–vector products. Thus, we can express the overall cost function $C(N)$ as

$$C(N) = T_s(N)/T = c_1\mathrm{NR}\cdot N\log N + c_2\mathrm{NR}\cdot\mathrm{LIN}\cdot N, \tag{70}$$

where c_1 and c_2 are fitting parameters. One can see from Fig. 12 that for moderately large number of cells, the ratio T_s/T increases according to the $\mathcal{O}(N\log N)$ scaling expected for the computation of the demagnetizing field by the 3D FFT convolution, whereas, for larger number of cells, the computational cost of the GMRES iterations becomes prevalent. In addition, as it was emphasized at the end of Section 5, if one disregards the magnetostatic field, the iterative procedure (56) becomes a pure Newton–Raphson algorithm which converges to the solution quadratically, leading to even shorter simulation times.

Finally, it is important to underline that by increasing the time-step Δt, the numerical algorithm exhibits a considerable speed-up, as one can see comparing the ratios T_s/T obtained in both the cases for a given number of cells $N = 6400$ and time-steps such that $(\gamma M_s)^{-1}\Delta t = 1, 2.5, 5$ ps. In all the simulations it has been observed that the relative error $e_{\alpha,\max}$ is in the order of 10^{-7}.

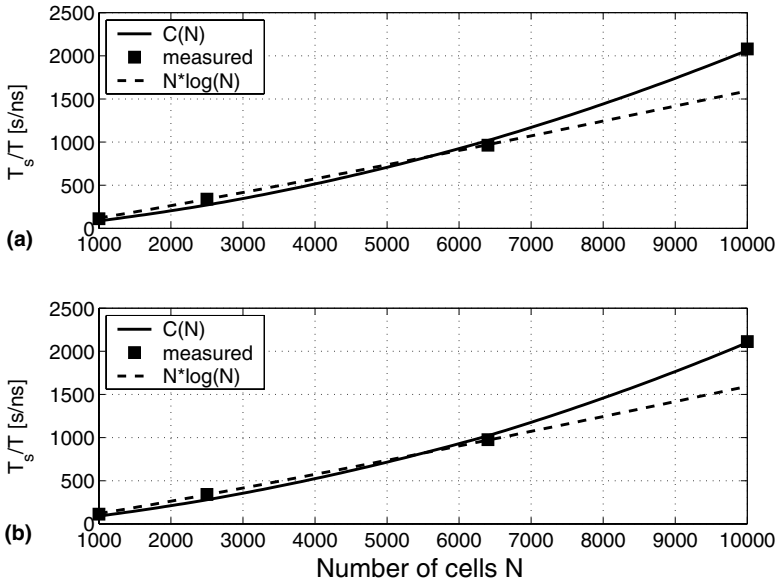

Fig. 12. Computational cost for μ-mag standard problem no. 4. Plots of the ratio T_s/T between simulation time T_s [s] and simulated time T [ns] for different number of cells N. The theoretical computational cost function $C(N)$ (solid line) and $N \log N$ scaling (dashed line) are also reported. The time-step is such that $(\gamma M_s)^{-1}\Delta t = 2.5$ ps. (a) $\delta = 170°$, $c_1 = 5 \times 10^{-4}$, $c_2 = 5.2 \times 10^{-4}$; (b) $\delta = 190°$, $c_1 = 6 \times 10^{-4}$, $c_2 = 4.8 \times 10^{-4}$.

9. Conclusions

In this paper, we have shown that the well-known mid-point rule technique can be successfully used for accurate micromagnetic simulations. In fact, mid-point rule allows one to obtain the preservation of the fundamental properties of the LLG dynamics: conservation of magnetization magnitude, Lyapunov structure and energy balance properties. The numerical results discussed in the paper show that the mid-point rule leads to an accurate reproduction of the precessional part of magnetization motion, which is very important in reversal processes. In addition, the mid-point rule technique can be applied to any spatial discretization which leads to the formal structure (26) of the effective field. In this respect, both finite difference and finite element methods [15] can be used. We have also shown that, for finite difference spatial discretization, the adoption of mid-point time-stepping leads to a feasible computational cost. In fact, despite the implicit nature of the mid-pint rule, the use of suitable quasi-Newton iterative procedure and fast iterative techniques to solve sparse linear systems (GMRES) leads to reasonable simulation times. This is also due to the fact that one can choose the time-step only for accuracy requirements, since the mid-point rule is unconditionally stable. The stability property of mid-point rule permits one to use a time-step comparable with the time scale of actual magnetization dynamics phenomena (ps).

Acknowledgment

This work is partially supported by the Italian MIUR-FIRB under contract no. RBAU01B2T8 and by ISI Lagrange Fellow Program.

References

[1] A. Aharoni, Introduction to the Theory of Ferromagnetism, Oxford University Press, 2001.
[2] G. Albuquerque, J. Miltat, A. Thiaville, Self-consistency based control scheme for magnetization dynamics, J. Appl. Phys. 89 (2001) 6719.
[3] M.A. Austin, P.S. Krishnaprasad, Almost Poisson integration of rigid body systems, J. Comput. Phys. 107 (1993) 105.
[4] M.N. Baibich, J.M. Broto, A. Fert, F. Nguyen Van Dau, F. Petroff, P. Etienne, G. Creuzet, A. Friederich, J. Chazelas, Giant magnetoresistance of (001)Fe/(001)Cr magnetic superlattices, Phys. Rev. Lett. 61 (1988) 2472–2475.
[5] D.V. Berkov, K. Ramstöck, A. Hubert, Solving micromagnetic problems: towards an optimal numerical method, Phys. Status Solidi A 137 (1993) 207.
[6] G. Bertotti, Hysteresis in Magnetism, Academic Press, San Diego, 1998.
[7] G. Bertotti, C. Serpico, I.D. Mayergoyz, Nonlinear magnetization dynamics under circularly polarized field, Phys. Rev. Lett. 86 (2001) 724.
[8] G. Binasch, P. Gruenberg, F. Saurenbach, W. Zinn, Enhanced magnetoresistance in layered magnetic structures with antiferromagnetic interlayer exchange, Phys. Rev. B 39 (1989) 4828–4830.
[9] A. Bloch, P.S. Krishnaprasad, J.E. Marsden, T.S. Ratiu, The Euler–Poincaré equations and double bracket dissipation, Commun. Math. Phys. 175 (1996) 1–42.
[10] W.F. Brown Jr., Micromagnetics, Interscience Publishers, 1963.
[11] C.J. Budd, M.D. Piggott, Geometric integration and its applications, <http://www.maths.bath.ac.uk/c~jb/>, 2001.
[12] P.J. Channell, J.C. Scovel, Symplectic integration of Hamiltonian systems, Nonlinearity 3 (1990) 231–259.
[13] M. Daniel, R. Amuda, Nonlinear dynamics of weak ferromagnetic spin chains, J. Phys. A: Math. Gen. 28 (1995) 5529–5537.
[14] J.M. Daughton, Magnetoresistive Random Access Memory (MRAM) Technology, February 4, 2000, <http://www.nve.com/otherbiz/mram.php>.
[15] J. Fidler, T. Schrefl, Micromagnetic modelling – the current state of the art, J. Phys. D: Appl. Phys. 33 (2000) R135.
[16] T.L. Gilbert, A Lagrangian formulation of the gyromagnetic equation of the magnetic field, Phys. Rev. 100 (1955) 1243.
[17] T.L. Gilbert, A phenomenological theory of damping in ferromagnetic materials, IEEE Trans. Magn. 40 (2004) 3443–3449.
[18] L.V. Kantorovich, G.P. Akilov, Functional Analysis, Pergamon Press, Oxford, 1982.
[19] R. Kikuchi, On the minimum of magnetization reversal time, J. Appl. Phys. 27 (1956) 1352.
[20] P.S. Krishnaprasad, X. Tan, Cayley transforms in micromagnetics, Physica B 306 (2001) 195.
[21] D. Lewis, N. Nigam, Geometric integration on spheres and some interesting applications, J. Comput. Appl. Math. 151 (2003) 141.
[22] C.S. Liu, Lie symmetry of the Landau–Lifshitz–Gilbert equation and exact linearization in the Minkowski space, Z. Angew. Math. Phys. 55 (2004) 606–625.
[23] D.P. Landau, M. Krech, Spin dynamics simulations of classical ferro- and antiferromagnetic model systems: comparison with theory and experiment, J. Phys.: Condens. Matter 11 (1999) R179–R213.
[24] J.C. Mallinson, Damped gyromagnetic switching, IEEE Trans. Magn. 36 (2000) 1976.
[25] J.E. Marsden, T.S. Ratiu, Introduction to Mechanics and Symmetry, Springer Verlag, New York, 1999.
[26] P.B. Monk, O. Vacus, Error estimates for a numerical scheme for ferromagnetic problems, SIAM J. Numer. Anal. 36 (3) (1998) 696–718.
[27] P.B. Monk, O. Vacus, Accurate discretization of a nonlinear micromagnetic problem, Comput. Methods Appl. Mech. Eng. 190 (40–41) (2001) 5243–5269.
[28] μ-mag group website, <http://www.ctcms.nist.gov/r~dm/mumag.org.html>.
[29] J.M. Ortega, W.C. Rheinboldt, Iterative Solution of Nonlinear Equations in Several Variables, SIAM, Philadelphia, PA, 2000.
[30] P. Podio-Guidugli, On dissipation mechanisms in micromagnetics, Eur. Phys. J. B 19 (2001) 417.
[31] A. Prohl, Computational Micromagnetism, Volume Xvi of Advances in Numerical Mathematics, Teubner, Leipzig, 2001.
[32] Y. Saad, M.H. Schultz, GMRES: a generalized minimal residual algorithm for solving nonsymmetric linear systems, SIAM J. Sci. Statist. Comput. 7 (3) (1986) 856.
[33] V.L. Safonov, H.N. Bertram, Intrinsic mechanism of nonlinear damping in magnetization reversal, J. Appl. Phys. 87 (2000) 5508.
[34] M.E. Schabes, A. Aharoni, Magnetostatic interaction fields for a three-dimensional array of ferromagnetic cubes, IEEE Trans. Magn. 23 (6) (1987).
[35] W. Scholz, PhD Thesis, <http://magnet.atp.tuwien.ac.at/scholz/>, 2003.
[36] C. Serpico, I.D. Mayergoyz, G. Bertotti, Analytical solutions of Landau–Lifshitz equation for precessional switching, J. Appl. Phys. 93 (2003) 6909.
[37] C. Serpico, I.D. Mayergoyz, G. Bertotti, Numerical technique for integration of the Landau–Lifshitz equation, J. Appl. Phys. 89 (2001) 6991.
[38] M. Slodička, L'. Bañas, A numerical scheme for a Maxwell–Landau–Lifshitz–Gilbert system, Appl. Math. Comput. 158 (2004) 79–99.
[39] M. Slodička, I. Cimrák, Numerical study of nonlinear ferromagnetic materials, Appl. Numer. Math. 46 (1) (2003) 95–111.

[40] A.W. Spargo, P.H.W. Ridley, G.W. Roberts, Geometric integration of the Gilbert equation, J. Appl. Phys. 93 (2003) 6805.
[41] D. Wang, M. Tondra, A.V. Pohm, C. Nordman, J. Anderson, J.M. Daughton, W.C. Black, Spin dependent tunneling devices fabricated for magnetic random access memory applications using latching mode, J. Appl. Phys. 87 (9) (2000) 6385.
[42] X. Wang, C.J. García-Cervera, E. Weinan, A Gauss-Seidel projection method for micromagnetics simulations, J. Comput. Phys. 171 (2001) 357–372.
[43] D. Weller, Assault on storage density of 1 Terabit/sq-in and beyond, in: Plenary Lecture at JEMS'04 Conference, Dresden, September 2004.
[44] P.E. Wigen, Nonlinear Phenomena and Chaos in Magnetic Materials, World Scientific Publishing, 1994.
[45] S.W. Yuan, H. Neal, Bertram, Fast adaptive algorithms for micromagnetics, IEEE Trans. Magn. 28 (1992) 2031.